

Umeå University

This is an accepted version of a paper published in *Carbon*. This paper has been peer-reviewed but does not include the final publisher proof-corrections or journal pagination.

Citation for the published paper:

Yu, J., Tonpheng, B., Gröbner, G., Andersson, O. (2011)

"Thermal properties and transition studies of multi-wall carbon nanotube/nylon-6 composites"

Carbon, 49(14): 4858-4866

URL: <http://dx.doi.org/10.1016/j.carbon.2011.07.006>

Access to the published version may require subscription.

Permanent link to this version:

<http://urn.kb.se/resolve?urn=urn:nbn:se:umu:diva-45835>

<http://umu.diva-portal.org>

**Thermal properties and transition studies of multi-wall carbon nanotube/nylon-6
composites**

Junchun Yu¹, Bounphanh Tonpheng¹, Gerhard Gröbner² and Ove Andersson^{1*}

¹Department of Physics, Umeå University, 901 87 Umeå, Sweden

²Department of Chemistry, Umeå University, 90187 Umeå, Sweden

*Corresponding author. Tel: +46 90 7865034; Fax: +46 90 7866673.
E-mail address: ove.andersson@physics.umu.se (O. Andersson)

Abstract

Transition behavior and thermal properties of a multi-wall carbon nanotube (MWCNT) /nylon-6 composite (P-composite) made by in-situ polymerization and subsequently structurally modified by high-pressure high-temperature treatment have been established. The thermal conductivity (κ) of nylon-6 improved $\sim 27\%$ by the addition of 2.1 wt % MWCNT filler simultaneously as the heat capacity per unit volume decreased $\sim 22\%$ compared with that of nylon-6 at 1 atm and 298 K. Moreover, the MWCNT filler raises the glass transition temperature (T_g) of nylon-6, but the pressure dependence of T_g remains unchanged. A model for κ indicates that the interfacial thermal resistance between the MWCNT filler and the nylon-6 matrix decreases 20% up to 1 GPa and most significantly above 0.8 GPa. P-composite was structurally modified by a sluggish cold-crystallization transition at 1.0 GPa, 530 K, which further increased κ by as much as $\sim 37\%$ as the crystallinity of nylon-6 improved from 31% to 58% with a preferred crystal orientation and increased crystal size.

1. Introduction

Carbon nanotubes (CNTs) have attracted intensive attention after the publications by Iijima [1, 2], which made this carbon structure common knowledge in the scientific community. CNTs are interesting because of their nano-sized diameter and micrometer length in combination with extraordinary thermal and mechanical properties, and high electrical conductivity. This gives CNTs a great potential to be utilized in thermal management, high performance composites, electronics etc [3]. Since our work here focuses on their potential to enhance the thermal properties of a polymer matrix, the thermal properties of CNTs are of particular interest. The CNT family is naturally subdivided into single-wall carbon nanotubes (SWCNTs) and multi-wall carbon nanotubes (MWCNTs), which may have somewhat different thermal properties. The thermal conductivity (κ) of SWCNTs and MWCNTs has been studied both experimentally and theoretically. Fujii et al. [4] measured κ of individual SWCNTs and found $\kappa > 2000 \text{ W m}^{-1} \text{ K}^{-1}$ for a CNT with a diameter of 9.8 nm, which further increased with decreasing diameter. Kim et al. [5] reported $\kappa > 3000 \text{ W m}^{-1} \text{ K}^{-1}$ for individual MWCNT at room temperature while that of bundled CNTs has been reported as $\sim 35 \text{ W m}^{-1} \text{ K}^{-1}$ for randomly orientated SWCNTs, $\sim 200 \text{ W m}^{-1} \text{ K}^{-1}$ for aligned SWCNTs and $\sim 20 \text{ W m}^{-1} \text{ K}^{-1}$ for randomly oriented MWCNTs [6-9]. Theoretically, it has been predicted that κ of a CNT can be as high as $\sim 7000 \text{ W m}^{-1} \text{ K}^{-1}$ at room temperature [10, 11]. Thus, adding relatively small amount of CNTs may dramatically improve κ of poor thermal conductors such as polymers. Especially since their high aspect ratio promotes percolation at low mass fractions. Their large specific surface area should also be beneficial for the thermal contact with a polymer matrix. Although results for CNT polymer composites show

strong improvement of κ at low CNT content, it is still significantly less than predicted by simple mixture rules and the reason is probably due to interfacial thermal resistance between the CNTs and the polymer matrix [12]. In this context, it is interesting to note that Haggemueller et al. [13] found 600% increase of κ by adding 20 vol % SWCNTs in high density polyethylene and that the increase was stronger than that predicted by a linear dependence on the SWCNT content. The latter suggests a percolation effect and Haggemueller et al. [13] surmised that this could be due to a well-conducting network of CNTs supported by crystalline bridges of polyethylene, which can nucleate and grow on CNTs.

In this study, we explore the change in interfacial thermal resistance between MWCNT and a nylon-6 matrix caused by crystallization under high pressure conditions and by high pressure densification as well as by temperature change. To the best of our knowledge, this is the first study of the effect of strong densification on the thermal contact between CNTs and a crystalline polymer. We have previously shown that treatment of nylon-6 under high-pressure high-temperature conditions causes a cold-crystallization transition, which significantly improves the degree of crystallinity concurrently as it induces a preferred orientation and increased lamellae size [14]. We have here chosen to study MWCNTs in nylon-6 because of their better dispersibility and the relative ease of purifying MWCNTs to a high degree of purity. In addition to their influence of κ , we report their effect on the heat capacity and transition behavior of nylon-6.

2. Experimental section

2.1. Materials and pre-treatment

MWCNTs produced by catalytic chemical vapor deposition were purchased from Nanocyl (3150 and 3151). Transmission electron microscopy analyses showed that Nanocyl 3150 and 3151 had average lengths of $\sim 1\mu\text{m}$ and $\sim 0.5\mu\text{m}$, respectively. Nanocyl 3151 (F-MWCNTs) with less than 4% of $-\text{COOH}$ functionalized MWCNTS, and a stated carbon purity of $>95\%$ and a metal oxide content of $<5\%$, was used without further purification. Nanocyl 3150 (P-MWCNTs) with a carbon purity of $>95\%$ and a metal oxide content of $<5\%$ was further purified before use. A typical purification procedure included oxidation in air, washing in 37% HCl acid (Sigma-Aldrich, ACS reagent) and, subsequently, rinsing by de-ionized and purified water (Milli-Q[®] Ultrapure WaterSystem), filtration and drying [15].

2.2. Synthesis of MWCNT/nylon-6 composites and nylon-6

The synthesis of the MWCNT/nylon-6 composites followed the steps suggested by Gao et al. [16, 17]: P-MWCNTs or F-MWCNTS (0.24 g) and 10 g ϵ -caprolactam (Aldrich, 99%) were loaded into a 50 mL three-neck round-bottom flask. The mixture was first sonicated with an ultrasonic bath (35 kHz, Bandelin Sonorex[®] RK 52H) for 30 min followed by sonication with ultrasonic pin (VCX 130, Sonics & Materials, INC.) for 90 min (50% power, pulse 20s on 20s off) at 80 °C. Subsequently, 1 g 6-aminocaproic acid (Sigma, $\geq 99\%$) was added to the suspension and the flask was transferred to a pre-heated silicon oil bath kept at 100 °C. The suspension was heated to 250 °C with mechanical stirring under dry nitrogen atmosphere and kept under these conditions for 6 h before cooling to room temperature. The cold sample was transferred to a nitrogen filled bag and

spooned out after slight heating. In order to remove un-reacted monomers and low molecular weight oligomers, the collected sample was cleaned by ultrasonic treatment in water at 80 °C for 1 hour. Finally, the washed sample was dried by vacuum pumping at 80 °C for 48 h. The 2.1 wt% F-MWCNTs/nylon-6 composite was prepared for promoting the possibility of covalent bonding between the filler and the matrix at HP&HT conditions. (-COOH groups of the functionalized MWCNTs could react with -NH₂ in nylon-6.) But the subsequent analysis of the HP&HT treated sample showed no signs of covalent bonds between F-MWCNT and nylon-6 (see supplementary material).

A control sample of nylon-6 without MWCNTs was synthesized using a similar procedure as for the composite: 12 g ε-caprolactam and 1.2 g 6-aminocaproic acid were loaded into a 50 mL three-neck round-bottom flask before it was mounted to a pre-heated silicon oil bath kept at 100 °C. The subsequent steps were the same as described above. The chemical structure of the synthesized nylon-6 and 2.1 wt% P-MWCNT/nylon-6 composite were confirmed by Fourier transform infrared spectroscopy (FTIR) and 2.1 wt% F-MWCNT/nylon-6 composite was examined by nuclear magnetic resonance (see supplementary material). The final product of nylon-6 had a viscosity-average molecular weight of 28 000 as determined by falling-ball viscometry (Thermo Scientific HAAKE falling ball viscometer type B).

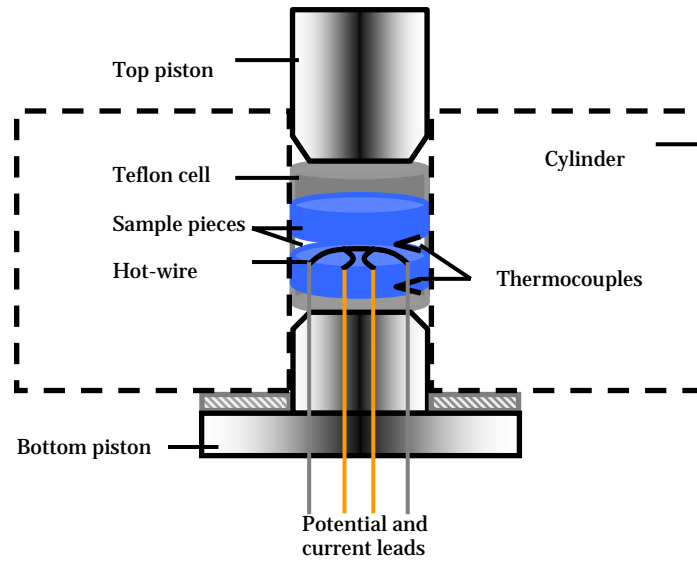


Fig. 1 - Schematic plot of the high-pressure setup

2.3. Experimental procedure and setup for hot-wire measurements

The MWCNT/nylon-6 composite and nylon-6 samples were hot pressed into plates (diameter: ~37 mm, thickness: ~ 3 mm) at 250 °C in an argon atmosphere, and degassed at 80 °C for 24 h in a vacuum oven before being assembled in a custom made Teflon cell. The Teflon cell, containing type K thermocouples and a hot-wire probe (0.1 mm Ni-wire) was mounted in a piston cylinder apparatus (Fig.1), which was transferred to a hydraulic press for high pressure, in-situ, hot-wire measurements [14]. The κ and heat capacity per unit volume (ρc_p) were measured simultaneously by the transient hot-wire method, with estimated inaccuracies of $\pm 2\%$ in κ and $\pm 5\%$ in ρc_p [18]. The pressure inaccuracy was estimated as ± 40 MPa at 1 GPa. (The pressure gradient in the probed sample volume of a few mm from hot-wire was significantly less.) During isobaric runs, the pressure was kept to within ± 1 MPa while the sample could be heated up to ca. 530 K by an electric heater surrounding the cylinder or cooled down to ca. 100 K by liquid nitrogen.

2.4. Crystallinity by Differential scanning calorimetry (DSC) and Wide Angle X-ray Diffraction (WAXD)

A Pyris Diamond DSC equipped with intra-cooler was used for DSC measurements. All the samples used for the DSC measurement were pumped 24 h in a vacuum oven and encapsulated under nitrogen atmosphere at room temperature to remove water and oxygen. The samples were heated from 20 to 250 °C at scan rate of 10 °C per minute and held at 250 °C for 5 minutes to ensure that the samples were melted before cooling to 20 °C by the same rate. The degree of crystallinity of the sample (C_{DSC}) was estimated from the heat of fusion [14]. WAXD was carried out using a Siemens/Bruker D5000 diffractometer with $CuK\alpha$ radiation at an acceleration voltage of 40 KV and a tube current of 30 mA. The samples were scanned from 5° to 50° (2θ) at scanning rate of 4° per minute. The degree of crystallinity of the sample (C_{WAXD}) was calculated from the areas of the crystalline and amorphous peak intensities [14]. The crystallinity presented in this paper, $C_{average}$, is an average of C_{DSC} and C_{WAXD} ($C_{average}=1/2\cdot(C_{DSC}+C_{WAXD})$).

2.5. Atomic force microscopy (AFM) and transmission electron microscopy (TEM)

AFM analysis of the P-MWCNT/nylon-6 composite using tapping mode was carried out by a MultiMode AFM (Nanoscope IV Controller, Veeco Metrology) equipped a LTESP probe (Veeco probe). The composite sample was dropped cast from melt on a silicon wafer. TEM (JEM-1230(Jeol)) equipped camera (Gatan MSC 600CW) was used for imaging P-MWCNTs at 80 KV. The P-MWCNTs was dispersed in ethanol using sonication for 5 minutes, and a small amount of the mixture was dropped on a copper grid and left in air for drying before the TEM analysis.

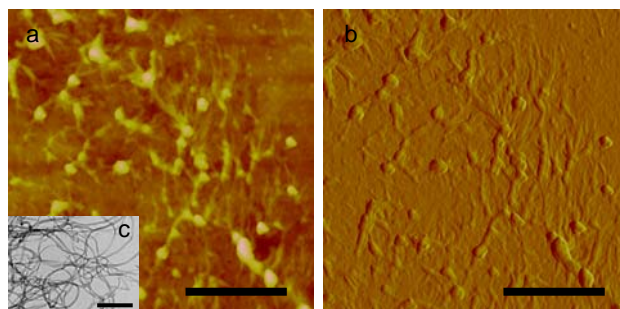


Fig. 2 - AFM image of P-MWCNT/Nylon-6 composite: (a) height image, (b) amplitude image (scale bar is 1 μm). The insert (c) is a TEM image of the purified P-MWCNTs (scale bar is 200 nm).

As shown in Fig. 2, height and amplitude images of the 2.1 wt% P-MWCNT/nylon-6 composite (P-composite) suggest a fairly good dispersion of P-MWCNTs in the nylon-6 matrix. The long, tubular and twisted structures, are polymer coated P-MWCNT or bundles, having a typical diameter of ~ 50 nm. A TEM image of purified P-MWCNTs (Fig. 2c) shows a diameter of ~ 12 nm but no amorphous carbon or metallic catalyst.

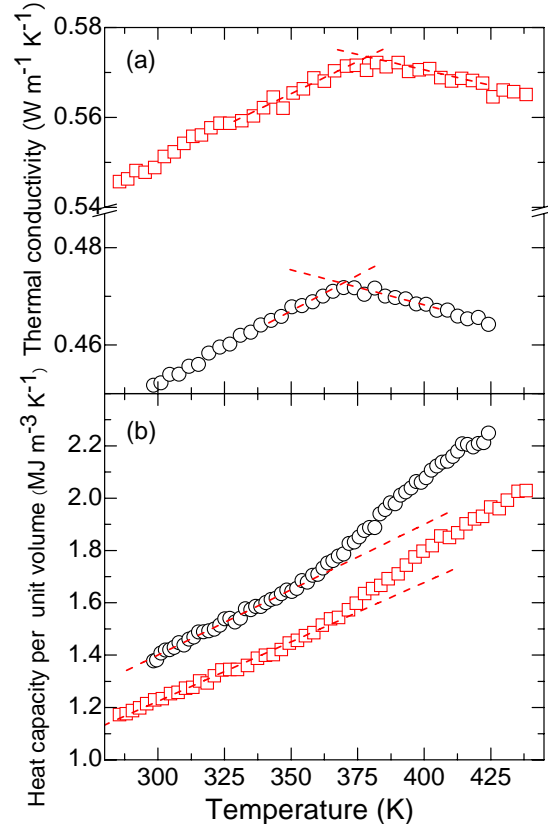


Fig. 3 - (a) Thermal conductivity and (b) heat capacity per unit volume of P-composite (\square) and nylon-6 (\circ) measured on heating at 0.8 GPa. The dashed red lines in (a) are linear fits of data below and above the slope change of the curve, which is associated with T_g . The dashed red lines in (b) represent linear fits below T_g .

3. Results and discussion

3.1. Glass transition behavior of nylon-6 and MWCNT/nylon-6 composite

Nylon-6 is known to show only weak or no changes in properties at its glass transition temperature (T_g) which occurs near 325 K for dry nylon-6 [19]. But we have recently reported a rather distinct change in $\kappa(T)$ at T_g of 319.6 K for (commercial) nylon-6 [14], for which κ changes from increasing below T_g to decreasing above. This T_g feature is typical for polymers [20] and made it possible to establish the pressure induced change of T_g for nylon-6. Fig. 3 shows that the same behavior occurs for 2.1 wt% P-

MWCNT/nylon-6 composite (P-composite) and our synthesized nylon-6, which has been briefly discussed previously [21], and it was also observed for 2.1 wt% F-MWCNT/nylon-6 composite (F-composite). The change of T_g caused by pressure densification was mapped by isobaric measurements for pressures up to 1.0 GPa. In general, the samples were heated to above T_g before the measurements commenced to avoid significant thermal history effects caused by pressurizing or depressurizing below the glass transition. Moreover, to avoid irreversible structural transformations like cold-crystallization, which significantly increases the degree of crystallinity [14], the samples were not heated above 400 K at pressures below 0.5 GPa or above 450 K at higher pressures until $T_g(p)$ had been established.

As shown in Fig. 3, κ of the P-composite and nylon-6, increases weakly on heating in the low temperature range. At T_g , the thermal expansivity increases, which causes the rather abrupt change in the temperature derivative of $\kappa(T)$ [14, 20]. Concurrently, the configurational heat capacity increases, and therefore also the ρc_p rises, as shown in Fig. 3b. Thus, this increase corresponds to the commonly observed (stretched) sigmoidal increase in the heat capacity, which is characteristic of glass transitions. It is normally more distinct, but the weak change observed for nylon-6 is consistent with the weak glass transition features reported in other properties [22]. The additional increase in the ρc_p at T_g , which gives a deviation from a linear extrapolation of the results at low temperatures (lines in Fig. 3b), agrees with the onset of the slope change in $\kappa(T)$, but it is somewhat less distinct. The results for T_g presented here (Fig. 4), which pertain to a time scale of 1 s [23], were obtained from the interception of the linear extrapolations of $\kappa(T)$ in the temperature ranges slightly below and above T_g , respectively. (As shown in Fig. 5, at

temperatures well above T_g , κ again weakly increases. Since the increase was reversible, we can exclude that this was due to a sluggish crystallization process and instead conclude that new phonon modes probably start to contribute to κ at high temperatures.)

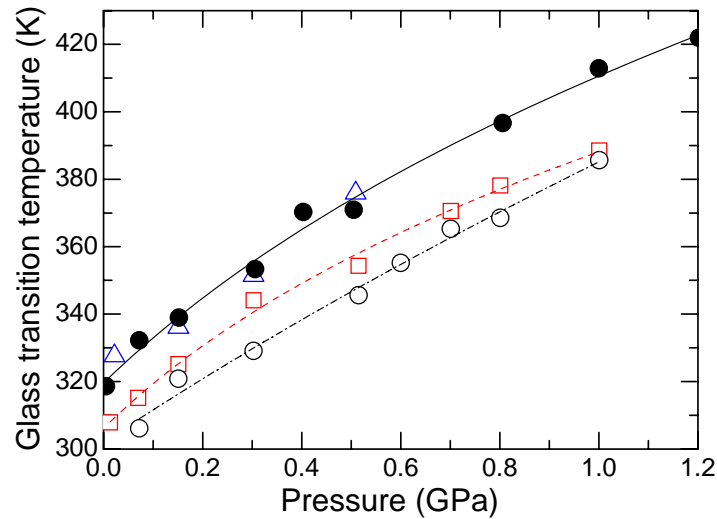


Fig. 4 - Glass transition temperature plotted against pressure: (\square) P-composite, (Δ) F-composite, (\circ) nylon-6 and (\bullet) commercial nylon-6 from Ref 14. The dashed lines for P-composite and nylon-6 represents fitted functions (Eq. 1). Probe failure prevented T_g measurements of the F-composite above 0.5 GPa.

The results for $T_g(p)$ of the two composites and nylon-6 (Fig. 4), which were extracted from the results for $\kappa(T)$, follow about the same pressure dependence. Considering the uncertainty in the determination of T_g , these seem shifted by roughly a constant temperature difference. Both the P- and F-composites show higher T_g than our synthesized nylon-6. In particular, T_g of the F-composite is in average shifted to ~ 10 K higher temperatures than that of the P-composite and by ~ 25 K compared to our synthesized nylon-6.

The changes of T_g with pressure are described well by the empirical equation [24]:

$$T_g(p) = T_0 \left(1 + \frac{b}{a} p \right)^{1/b} \quad (1)$$

where a , b and T_0 are fitting parameters, and p is the pressure in GPa. For nylon-6, we find: $T_0 = 302.1$ K, $a = 2.22$ GPa and $b = 3.11$; and for the P-composite the fit yielded: $T_0 = 306.1$ K, $a = 2.11$ GPa and $b = 5.29$. (The few values determined for the F-composite make its fitting parameters less reliable and those are therefore not given.) Apparently, T_g of our synthesized nylon-6 is lower than the typically reported literature values of about 325 K [19], which we attribute to higher water content in our nylon-6 sample.

Iwamoto and Murase [25] have studied the interaction between nylon-6 and water by FTIR during dehydration. They found that water interacts with amide groups in the amorphous part of nylon-6 to form hydrogen bonds with non-hydrogen bonded or free C=O or NH, which give characteristic features in FTIR spectra. However, we could not find any of these features in the FTIR spectrum of nylon-6 (supplementary material), suggesting that there is no massive amount water. It is well known that the moisture content significantly affects T_g of nylon-6, which has been studied in detail by Khanna et al. [26]. If one disregards sample differences, e.g. molecular weight which was not given by Khanna et al. [26], then their results imply that T_g of 319.6 K for commercial nylon-6 at 1 atm [14] (Fig. 4) corresponds to a water content of ca. 0.2 wt%. This increases to ca. 1.0 wt% for our synthesized nylon-6 with T_g of 302.1 K. Thus, despite several water removal steps, including drying in vacuum oven for 48 h at 80 °C; melting and casting the samples in dry argon atmosphere, and vacuum pumping again for 24 h at 80 °C, about 1 wt% of water remained. All samples were subjected to identical treatments and were loaded in the sample cell under dry argon atmosphere, which should give about the same water content. We can therefore conclude that the MWCNT raises T_g of nylon-6, but due

to the unusually strong T_g dependence on the water content, it is difficult to reliably access the exact size of the increase. The results obtained here indicate a surprisingly large difference between the two composites, whereas the about 10 K higher T_g for the P-composite compared to that of pure nylon-6 sample is only somewhat larger than the few degrees typical reported when MWCNTs are added in a polymer matrix.

Coating or wrapping of CNTs by polymer is commonly observed in polymer/CNTs composite [27-29]. When CNTs are added to a polymer, T_g typically increases a few degrees [30, 31] but may also increase a few tenth of degrees [32]. Because of its nano-scaled tubular geometry, well dispersed and uniformly distributed MWCNTs in a polymer matrix likely act as obstacles for molecular rearrangements. In particular, if the chains become wrapped around the CNTs. In terms of the free volume theory, CNTs reduces the free space available for the chain rearrangements. Apart from a reduced free space caused by CNTs, pressurization causes an additional reduction, but the results obtain here shows that the effects of the CNTs is to simply raise T_g by a constant, pressure independent, temperature shift. That is, neither the MWCNTs nor the water content strongly affects the pressure dependence of T_g .

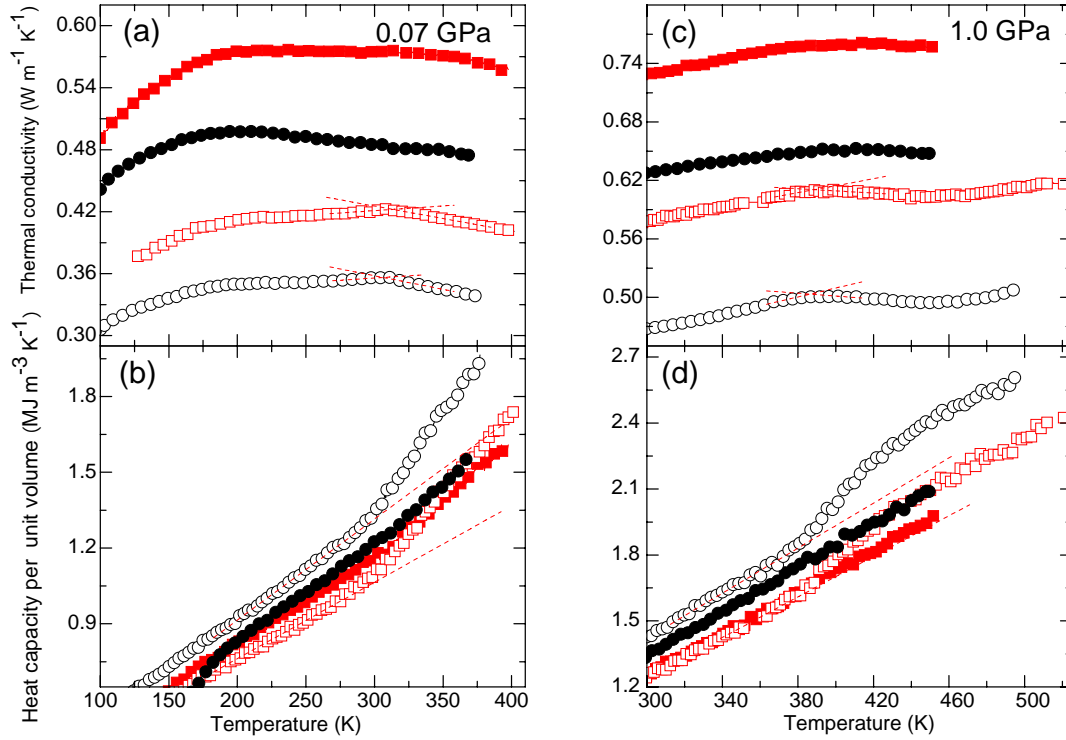


Fig. 5 - (a, c) Thermal conductivity and (b, d) heat capacity per unit volume measured on heating at 0.07 GPa and 1.0 GPa before (open symbols) and after (filled symbols) HP&HT treatment at 1.0 GPa and 530 K: (\square, \blacksquare) P-composite, and (\circ, \bullet) nylon-6. The dashed red lines in (a) and (c) are linear fits of data below and above the slope change of the curve, which is associated with T_g . The lines in (b) and (d) represent linear fits below T_g .

After HP&HT treatment at 1 GPa and 530 K (see experimental), the T_g features of the P-composite and nylon-6 vanished. (Several failures of the probe during the treatment of the F-composite prevented the study of its HP&HT treated state.) That is, the distinct change in $d\kappa/dT$ could not be observed and the slope of ρc_p remained unchanged on heating (Fig. 5). This is the same results as found previously for commercial nylon-6, which was established as due to a reduced amorphous fraction [14]. That is, the vanishing

of the T_g features implies an amorphous to crystalline structural conversion during the HP&HT treatment, which is also confirmed by the results for the degree of crystallinity discussed below.

3.2. Theoretical estimation of κ of composites

Several models have been proposed to predict κ of polymer based CNT composites for which the interfacial thermal contact resistance between the CNTs and the polymer has been found essential. Nan et al. [12, 33, 34] have derived a model for κ , which accounts for the interfacial thermal resistance in composites of randomly dispersed CNTs in a matrix. The interfacial resistance was accounted for by a thin coating of a poorly thermally conducting layer on the surface of the CNTs. Their expression for κ of the composite κ_{Com} is given by:

$$\frac{\kappa_{Com}}{\kappa_{Ny}} = 1 + \frac{fp}{3} \frac{\kappa_{MWCNTs} / \kappa_{Ny}}{p + \frac{2a_k}{d} \frac{\kappa_{MWCNTs}}{\kappa_{Ny}}} \quad (2)$$

where κ_{Ny} and κ_{MWCNT} are κ of nylon-6 ($0.33 \text{ W m}^{-1} \text{ K}^{-1}$) and MWCNT ($\sim 3000 \text{ W m}^{-1} \text{ K}^{-1}$) respectively; f (0.013) is the volume fraction of MWCNTs; $p=L/d$ (L is the length and d is the diameter of CNTs, $d=10 \text{ nm}$, L is $1 \text{ }\mu\text{m}$ and $0.5 \text{ }\mu\text{m}$ for P-MWCNTs and F-MWCNTs respectively); a_k is a so-called Kapitza radius defined by $a_k = R_k \cdot \kappa_{Ny}$ (R_k is Kapitza resistance [35]).

Fig. 6c shows that κ of the P-composite, with 2.1 wt% (0.013 vol%) of P-MWCNTs in nylon-6, is $\sim 0.42 \text{ W m}^{-1} \text{ K}^{-1}$ at 1 atm and 298 K, which is 27 % higher than that of nylon-6 ($0.33 \text{ W m}^{-1} \text{ K}^{-1}$). Since the degree of crystallinity of the P-composite was about the same as that of nylon-6 (Table 1), the higher κ of the P-composite must be caused entirely by the MWCNT filler.

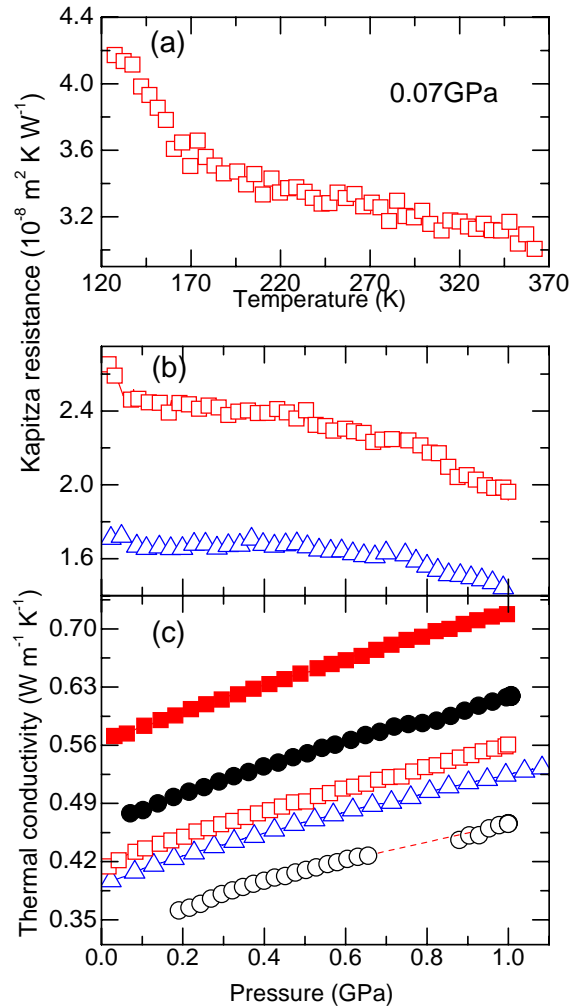


Fig. 6 - (a) Kapitza resistance plotted against temperature for the (\square) P-composite at 0.07 GPa. (b) Kapitza resistance plotted against pressure at 298 K for: (\square) P-composite and (Δ) F-composite. (c) Thermal conductivity plotted against pressure at 298 K before (open symbols) and after (filled symbols) HP&HT treatment for: (\square, \blacksquare) P-composite, (Δ) F-composites and (\circ, \bullet) nylon-6. The red dashed line shows a range where the data have been omitted due to influences by a transition in Teflon (sample cell material).

Table 1 - Average degree of crystallinity calculated from C_{DSC} and C_{WAXD} results (see experimental).

Sample	$C_{average}$
Virgin Nylon-6	30%
Nylon-6 treated at 1.0 GPa	56%
Virgin P-composite	31%
P-composite treated at 1.0 GPa	58%

If the interfacial resistance is ignored in the model ($a_k=0$), Eq. (2) reduces to $\kappa_{Com} = \kappa_{Ny} + \kappa_{MWCNTs} f / 3$, and κ becomes proportional to the fraction of MWCNTs, which yields $13.33 \text{ W m}^{-1} \text{ K}^{-1}$ at atmospheric pressure. This value is far from the measured value of $0.42 \text{ W m}^{-1} \text{ K}^{-1}$, which is likely due to interfacial thermal resistance and it is accounted for by a non-zero value of R_k in Eq. (2) At room temperature and atmospheric pressure, the results for the P- and F-composites imply $R_k = 2.5 \times 10^{-8} \text{ m}^2 \text{ K W}^{-1}$ and $1.7 \times 10^{-8} \text{ m}^2 \text{ K W}^{-1}$, respectively (This difference between R_k of the two composites is probably within the inaccuracy of the calculation. For example, it can be accounted for by a $\sim 30\%$ uncertainty in the aspect ratio.) Thus, the key for improving κ of CNT composites is to reduce the interfacial resistance and possibly obtain a percolation network of the highly thermally conducting CNTs. Zhong and Lukes [36] used molecular dynamics simulations to study the effect of CNT length, overlap and spacing on the interfacial resistance between two SWCNTs, and found that it decreases with increasing CNT overlap and length and decreasing inter-CNTs spacing. Within the framework of the model of Nan et al. [12], we have here used the possibility to calculate the changes in interfacial resistance with temperature and pressure in a CNT-polymer composite, which have not been studied before.

3.3. Temperature dependence of thermal conductivity

The results for $\kappa(T)$ of both pure nylon-6 and the P-composite, shown in Fig. 5, show identical and typical amorphous-like behavior, i.e. κ is low and only weakly temperature dependent. We can therefore conclude that $\kappa(T)$ of the P-composite is governed by that of nylon-6, which is amorphous-like despite a significant crystalline fraction. Since we have data for pure nylon-6 and its MWCNT composite, we can use literature data for the CNTs to calculate the change in the interfacial resistance on heating. (The $\kappa=3000 \text{ W m}^{-1} \text{ K}^{-1}$ of the MWCNTs was here assumed constant.) Based on Eq. (2), we find that R_k decreases on heating, as shown in Fig. 6a. In particular, R_k decreases strongly in the 120 to 170 K range, and then less pronounced on further heating, implying better phonon-phonon coupling at the MWCNTs/polymer interface near room temperature than at low temperatures. The results indicate that the interfacial resistance can become very large at temperatures well below 100 K, which is in correspondence with previous results for a 5 wt% Cu nanoparticle/nylon-6 composite [37]. In this case, κ of the composite was almost identical to that of nylon-6 in the temperature range 0.1 K to 30 K, which implies a very large thermal interfacial resistance between the Cu nanoparticles and the nylon-6 matrix at low temperatures. That is, the significant increase of the interfacial resistance observed here on temperature decrease is not specific for polymer-CNT composites.

3.4. Pressure dependence of thermal conductivity

All the samples were studied by pressure runs from low pressure up to 1 GPa at 298 K. As shown in Fig. 6c, κ increases with pressure, or decreasing interparticle distance (inter-CNT, CNT-chain and interchain). All the samples have similar but not identical $d\kappa/dp$, which is well described by linear functions. The function for nylon-6 is given by

$d\kappa_{Ny} / dp = 0.19 - 0.10p$ (p in GPa), which shows that the pressure induced increase of κ becomes weaker with increasing pressure. This is the normal behaviour as the densification levels off at high pressure and, thus, the reduction of the interchain distance becomes less pronounced. The corresponding results for the P- and F-composites are: $d\kappa_{P-com} / dp = 0.17 - 0.05p$ (p in GPa) and $d\kappa_{F-com} / dp = 0.15 - 0.04p$ (p in GPa), respectively, which suggest that the increase of κ for the composites is less weakened than that of nylon-6. The reason for this difference may be due to the positive effect of pressure on the CNT-CNT and CNT-chain interaction, which can be assessed by calculation of the interfacial resistance R_k (Eq. 2) as a function of pressure.

The results for R_k of the P- and F-composite are shown in Fig. 6b. Both results show that R_k decreases with increasing pressure, and the decrease for the P-composite is $\sim 20\%$ up to 1 GPa. It is interesting to note that the decrease accelerates at high pressures near 0.8 GPa, which indicates that the reduction of the interfacial contact resistance accelerates. Still, it is apparent that pressure achieved here for a MWCNT content of 2.1 wt% is insufficient to obtain a percolation network, i.e. the increase in κ on pressurization is mainly due to that associated with the nylon-6 matrix, at least up to pressures near 0.8 GPa.

Fig. 6c shows also $\kappa(p)$ of the P-composite and nylon-6 after the HP&HT treatment. The HP&HT treated samples show similar $d\kappa/dp$ behavior as the corresponding untreated samples, but with a higher initial κ . In this case, we can conclude that the increased degree of crystallinity from about 30% to near 60% did not significantly change the effect of pressure on κ and the results show no tendency of strongly increasing κ on pressure rise, which would indicate the initiation of a highly thermally conducting network.

3.5. Heat capacity of nylon-6 and MWCNT/nylon-6 composite

Fig. 5b shows the ρc_p of both nylon-6 and the P-composite. The value for nylon-6 at 298 K and 1 atm is about $1.3 \text{ MJ m}^{-3} \text{ K}^{-1}$, which was obtained by extrapolation of high pressure results. The value for the P-composite, however, is significantly lower and only $\sim 1.0 \text{ MJ m}^{-3} \text{ K}^{-1}$. If the MWCNTs can be treated as non-interacting particles in the nylon-6 matrix, then the heat capacity of the P-composite is given by the mixture rule. The mixture rule equations for density ρ_{Com} and specific heat capacity $c_{p,Com}$ are:

$$\rho_{Com} = \frac{1}{\frac{w_{Ny}}{\rho_{Ny}} + \frac{w_{MWCNTs}}{\rho_{MWCNTs}}} \quad (3)$$

$$c_{p,Com} = w_{Ny} c_{p,Ny} + w_{MWCNTs} c_{p,MWCNTs} \quad (4)$$

where w is the weight fraction of MWCNTs (2.1%). The density and specific heat capacity of MWCNT at room temperature and atmospheric pressure are $\sim 1.9 \text{ g cm}^{-3}$ [38] and $400 \text{ J kg}^{-1} \text{ K}^{-1}$ [9] respectively. These values together with the values for pure nylon-6 yields a ρc_p of $1.29 \text{ MJ m}^{-3} \text{ K}^{-1}$ for the 2.1 wt% MWCNT/nylon-6 composite, i.e. the experimental value for the P-composite of $1.0 \text{ MJ m}^{-3} \text{ K}^{-1}$ is 22% smaller. This indicates that MWCNTs suppress the heat capacity of the polymer matrix despite the weak van der Waals interaction between the MWCNTs and the nylon-6 matrix. The results are qualitatively similar to those obtained previously in a transient hot-wire study of a SWCNTs/polyisoprene composite [39]. In this case, 5 wt% SWCNTs caused a 30% decrease of the heat capacity. Moreover, one DSC study indicates a similar decrease for polystyrene with 5 wt% SWCNTs [40], but another reports essentially no change for a 2.5 wt% SWCNT/polystyrene composite [41]. A DSC study of 1 wt% SWCNTs in poly(methylmethacrylate) [42] also shows essentially the same heat capacity as the neat

polymer. These results call for further studies to determine the effect of CNTs on the heat capacity of polymers and the reason for the different results.

3.6. HP&HT transition and the effect on properties

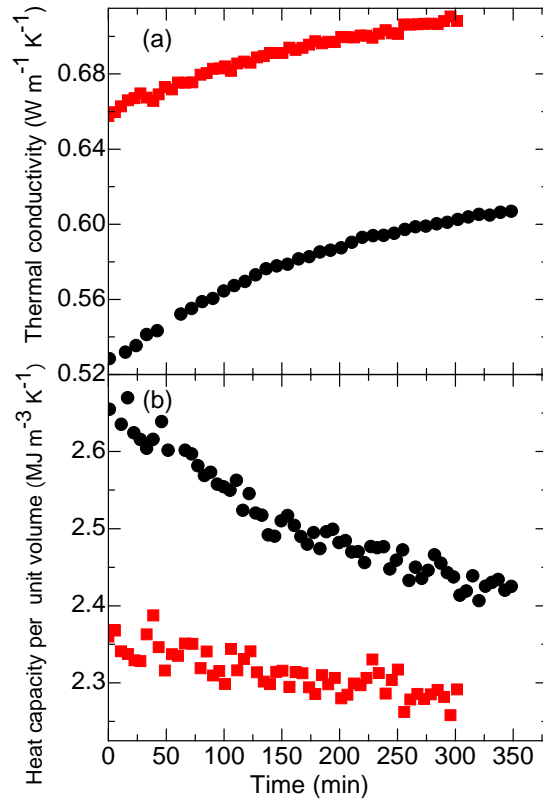


Fig. 7 - (a) Thermal conductivity and (b) heat capacity per unit volume plotted against time during treatment at 530 K and 1.0 GPa: (■) P-composite and (●) nylon-6. The slow change of the properties indicates a sluggish cold-crystallization transition.

A sluggish transition was detected through a time dependence in κ and the ρc_p when the samples were heated to ~ 530 K at 1 GPa (Fig. 7). The properties, which changed slowly with time t in an exponential manner, were fitted using a function of the type: $\exp(-t/\tau)$, where τ is the time constant. The fits yielded: $\kappa = 0.727 - 0.068 e^{-t/227}$ W m⁻¹ K⁻¹ and

$\rho c_p = 2.358 + 0.312e^{-t/216}$ MJ m⁻³ K⁻¹ for the P-composite (t in minutes). That is, the process had a time constant of ~ 3.7 h and caused κ to increase 8%, while ρc_p decreased 3% during 5 h. The corresponding process for nylon-6 had a time constant of ~ 3.6 h while κ increased 14% ($\kappa = 0.624 - 0.098e^{-t/198}$ W m⁻¹ K⁻¹) and ρc_p decreased 7% ($\rho c_p = 2.249 + 0.118e^{-t/237}$ MJ m⁻³ K⁻¹) during 5 h.

After the HP&HT treatment, the thermal properties were established as a function of pressure and temperature. The results show that the difference in properties before and after the HP&HT treatment depends strongly on the conditions. At 0.07 GPa and 298 K (Fig. 5a), κ of the P-composite increased from 0.420 to 0.575 W m⁻¹ K⁻¹ (37%) and ρc_p increased from 1.10 to 1.16 MJ m⁻³ K⁻¹ (5%). The corresponding results for nylon-6 (Fig. 5c) show an increase in κ from 0.356 to 0.485 W m⁻¹ K⁻¹ (36%) and a decrease in ρc_p from 1.32 to 1.21 MJ m⁻³ K⁻¹ (8%).

After the measurements, the samples were recovered at 1 atm and studied by DSC, WAXD, viscosity and FTIR measurements. As shown in Table 1, the samples showed a pronounced increase of crystallinity, from $\sim 31\%$ before treatment to $\sim 57\%$, after the HP&HT treatment, which is about the same as that found previously for similarly treated commercial nylon-6 [14]. A detailed analysis of WAXD and DSC data of the HP&HT treated commercial nylon-6 also showed that the crystal sizes increased and that the treatment promoted chain folding within the plane perpendicular to the applied load, i.e. the new and enlarged nylon-6 crystals had a preferred crystal orientation [14]. As WAXD and DSC results of our nylon-6 and P-composite were similar to those of commercial nylon-6, we conclude that their microstructure changed in the same manner as that of commercial nylon-6. Moreover, the viscosity results show that the HP&HT treatment

leads to slight chain scissoring where the average chain length decreased from 28 000 to 10 000. The FTIR results before and after treatment were the same except for more distinct crystalline feature in the spectra [22], which is due to the increased degree of crystallinity (see supplementary material).

The increase of κ for pure nylon-6 of about 14% during the transformation is due to the change of microstructure, i.e. the increased crystallinity with crystals of larger sizes and a preferred orientation. An amorphous structure strongly reduces the phonon mean free path whereas phonon transport in crystalline structures is normally limited by phonon-phonon scattering except at low temperatures. Polymers are special cases due to their characteristic microstructure. Heat transport along the polymer chains is high but the small crystal sizes with folded chains and inter-lamellae amorphous fractions strongly limit κ even in polymers with high degree of crystallinity. Thus, enhanced crystallinity increases κ , but the increase is not as pronounced as for other materials where κ can increase an order of magnitude or more at an amorphous to crystalline conversion.

In CNT-polymer composites, the highly thermally conducting CNTs ($\sim 10^4$ higher κ than the polymer) may show ballistic phonon propagation, at least at low temperatures [43], and provide highly conducting bridges in the polymer matrix. However, poor coupling between the vibration modes of the polymer and those of the CNTs gives apparently a large thermal resistance. The results here for the change of κ during HP&HT treatment show that an increase of crystallinity under densified conditions does not significantly improve or change the interfacial contact. Table 1 shows that the HP&HT treatment gives about the same increase of crystallinity for the composite as for pure nylon-6. Since the

increase of κ for the P-composite and nylon-6 is about the same, it is likely due mainly to the change of the nylon-6 microstructure.

3.7. Crystallinity dependence of thermal conductivity

One of the most important properties that affects κ of semicrystalline polymers is the degree of crystallinity. Choy and Young [44, 45] have proposed a model for estimation of κ of semicrystalline polymers, which they considered as a two-phase material with randomly oriented and roughly spherical crystallites embedded in an amorphous matrix. Their equation for calculation of the thermal conductivity of a semicrystalline nylon-6 sample κ_{Ny} is given by [45]:

$$\frac{\kappa_{Ny} - \kappa_a}{\kappa_{Ny} + 2\kappa_a} \cong C \left(\frac{2}{3} \frac{\kappa_{\perp} - 1}{\kappa_{\perp} + 2} + \frac{1}{3} \right) \quad (5)$$

where κ_a is the κ of amorphous nylon-6, $\kappa_{\perp} = \kappa_{c\perp} / \kappa_a$, where $\kappa_{c\perp}$ is the κ perpendicular to the chain direction of a crystallite, and C is the degree of crystallinity. In general, κ_{\perp} is close to 1, which is also the value adopted here [46].

We can now calculate a value for κ of amorphous nylon-6 pertaining to the molecular weight of our sample ($\sim 10^4$) at 298 K and 1 atm and also use Eq. (5) to predict a value of κ of the high crystalline HP&HT treated sample. The value for κ of nylon-6 measured here of $0.330 \text{ W m}^{-1} \text{ K}^{-1}$ at 298 K and 1 atm pertains to a crystallinity of 30%, which gives $\kappa_a = 0.248 \text{ W m}^{-1} \text{ K}^{-1}$. The crystallinity of our HP&HT treated nylon-6 of 56% inserted in Eq. (5) then yields $0.419 \text{ W m}^{-1} \text{ K}^{-1}$, which is 11% lower than the experimental value of $0.465 \text{ W m}^{-1} \text{ K}^{-1}$. A part or all of this difference can be due to the increase of the crystal sizes and the preferred crystal orientation caused by the HP&HT treatment, which is not accounted for by Eq. (5).

The κ of the treated P-composite can also be estimated using Eq. (5) and Eq. (2) by assuming that the interfacial thermal contact remains unchanged by the treatment. The κ of the nylon-6 matrix of the P-composite is obtained by inserting its crystallinity of 58% in Eq. (5), which gives $k_{Ny} = 0.424 \text{ W m}^{-1} \text{ K}^{-1}$. Thus, if the interfacial contact remains unchanged by the treatment then $R_k = 2.65 \times 10^{-8} \text{ m}^2 \text{ K W}^{-1}$, as shown in Fig. 6b, and Eq. (2) gives $\kappa = 0.505 \text{ W m}^{-1} \text{ K}^{-1}$ for the treated P-composite. This is 14% lower than the experimental value of $0.575 \text{ W m}^{-1} \text{ K}^{-1}$, which is about the same underestimate as that for pure nylon-6 (11%). We can therefore conclude that the increase of κ caused by the HP&HT treatment of the P-composite is due to the change in the nylon-6 microstructure, i.e. the increased degree of crystallinity with larger crystal sizes and preferred crystal orientation, with a minor contribution by improved interfacial contact.

4. Conclusions

The MWCNT filler induced changes of the thermal properties and glass transition temperature (T_g) of nylon-6 have been established in wide temperature and pressure ranges. The T_g increases a few degrees ($\sim 10 \text{ K}$) and the thermal conductivity of nylon-6 improves $\sim 27\%$ while the ρc_p decreases $\sim 22\%$ by the addition of 2.1 wt % MWCNT in nylon-6 (P-composite). The latter indicates that MWCNTs can significantly change the properties of the nylon-6 matrix even though it is generally regarded as an inert filler. The relatively weak increase of the thermal conductivity, despite the highly thermally conductive filler, is due to large interfacial thermal resistance between the MWCNTs and the polymer. The resistance increases with decreasing temperature but decreases with increasing pressure. The decrease is about 20% up to 1 GPa, and it is most significant above 0.8 GPa. Based on these results, we can conclude that pressure reduces the thermal

resistance but that the range achieved here for the P-composite is insufficient to obtain a highly thermally conducting network of MWCNTs, i.e., the increase in thermal conductivity on pressurization is mainly due to that associated with the nylon-6 matrix, at least up to pressures near 0.8 GPa.

A sluggish cold crystallization transformation was observed in both nylon-6 and the P-composite at ~530 K and 1.0 GPa. As a result, the degree of crystallinity of the P-composite increased from 31% to 58% and all glass transition features vanished. The new and more ordered state of the P-composite has about 37% higher thermal conductivity than the virgin state, which is mostly due to the change of the nylon-6 microstructure, i.e. a significantly increased degree of crystallinity with larger crystal sizes and a preferred crystal orientation. The thermal conductivity enhancement appears to be limited by a large thermal resistance at the amorphous inter-lamellae fractions as well as at the MWCNT-nylon-6 interfaces.

Acknowledgement

We are grateful for financial support from Magn. Bergvalls foundation and SIDA/SAREC.

References

- [1] Iijima S. Helical microtubules of graphitic carbon. *Nature* 1991; 354(6348):56-8.
- [2] Iijima S, Ichihashi T. Single-shell carbon nanotubes of 1-nm diameter. *Nature* 1993; 363(6430):603-5.
- [3] Moniruzzaman M, Winey KI. Polymer Nanocomposites Containing Carbon Nanotubes. *Macromolecules* 2006; 39(16):5194-205.
- [4] Fujii M, Zhang X, Xie H, Ago H, Takahashi K, Ikuta T, et al. Measuring the Thermal Conductivity of a Single Carbon Nanotube. *Phys Rev Lett* 2005; 95(6):065502.
- [5] Kim P, Shi L, Majumdar A, McEuen PL. Thermal Transport Measurements of Individual Multiwalled Nanotubes. *Phys Rev Lett* 2001; 87(21):215502.
- [6] Hone J. *Phonons and Thermal Properties of Carbon Nanotubes*. Berlin Heidelberg: Springer-Verlag; 2001: 273-86.

- [7] Hone J, Llaguno MC, Biercuk MJ, Johnson AT, Batlogg B, Benes Z, et al. Thermal properties of carbon nanotubes and nanotube-based materials. *Appl Phys A: Mater Sci Process* 2002; 74(3):339-43.
- [8] Yang DJ, Zhang Q, Chen G, Yoon SF, Ahn J, Wang SG, et al. Thermal conductivity of multiwalled carbon nanotubes. *Phys Rev B* 2002; 66(16):165440.
- [9] Yi W, Lu L, Dian-lin Z, Pan ZW, Xie SS. Linear specific heat of carbon nanotubes. *Phys Rev B* 1999; 59(14):R9015.
- [10] Berber S, Kwon Y-K, Tománek D. Unusually High Thermal Conductivity of Carbon Nanotubes. *Phys Rev Lett* 2000; 84(20):4613.
- [11] Donadio D, Galli G. Thermal Conductivity of Isolated and Interacting Carbon Nanotubes: Comparing Results from Molecular Dynamics and the Boltzmann Transport Equation. *Phys Rev Lett* 2007; 99(25):255502.
- [12] Nan C-W, Liu G, Lin Y, Li M. Interface effect on thermal conductivity of carbon nanotube composites. *Appl Phys Lett* 2004; 85(16):3549-51.
- [13] Haggemueller R, Guthy C, Lukes JR, Fischer JE, Winey KI. Single Wall Carbon Nanotube/Polyethylene Nanocomposites: Thermal and Electrical Conductivity. *Macromolecules* 2007; 40(7):2417-21.
- [14] Yu J, Tonpheng B, Andersson O. High-Pressure-Induced Microstructural Evolution and Enhancement of Thermal Properties of Nylon-6. *Macromolecules* 2010; 43(24):10512-20.
- [15] Moon J-M, An KH, Lee YH, Park YS, Bae DJ, Park G-S. High-Yield Purification Process of Singlewalled Carbon Nanotubes. *J Phys Chem B* 2001; 105(24):5677-81.
- [16] Gao J, Zhao B, Itkis ME, Bekyarova E, Hu H, Kranak V, et al. Chemical Engineering of the Single-Walled Carbon Nanotube-Nylon 6 Interface. *J Am Chem Soc* 2006; 128(23):7492-6.
- [17] Gao J, Itkis ME, Yu A, Bekyarova E, Zhao B, Haddon RC. Continuous Spinning of a Single-Walled Carbon Nanotube-Nylon Composite Fiber. *J Am Chem Soc* 2005; 127(11):3847-54.
- [18] Hakansson B, Andersson P, Backstrom G. Improved hot-wire procedure for thermophysical measurements under pressure. *Rev Sci Instrum* 1988; 59(10):2269-75.
- [19] Aharoni SM. *n-Nylons: their synthesis, structure, and properties*. Chichester: John Wiley & Sons, Ltd.; 1997:
- [20] Van Krevelen DW. *Properties of polymers: correlations with chemical structure*: Elsevier publishing company; 1972: 234.
- [21] Yu J, Tonpheng B, Andersson O. Thermal Conductivity and Heat Capacity of a Nylon-6/Multi-wall Carbon Nanotube Composite Under Pressure. *AIP Conf Proc* 2010; 1255(1):145-7.
- [22] Kohan MI. *Nylon Plastics Handbook*. Cincinnati: Hanser/Gardner Publications, Inc. ; 1995: 87-8.
- [23] Andersson O. Simulation of a glass transition in a hot-wire experiment using time-dependent heat capacity. *Int J Thermophys* 1997; 18(1):195-208.
- [24] Andersson SP, Andersson O. Relaxation Studies of Poly(propylene glycol) under High Pressure. *Macromolecules* 1998; 31(9):2999-3006.

- [25] Iwamoto R, Murase H. Infrared spectroscopic study of the interactions of nylon-6 with water. *J Polym Sci Part B: Polym Phys* 2003; 41(14):1722-9.
- [26] Khanna YP, Kuhn WP, Sichina WJ. Reliable Measurements of the Nylon 6 Glass Transition Made Possible by the New Dynamic DSC. *Macromolecules* 1995; 28(8):2644-6.
- [27] Tallury SS, Pasquinelli MA. Molecular Dynamics Simulations of Flexible Polymer Chains Wrapping Single-Walled Carbon Nanotubes. *J Phys Chem B* 2010; 114(12):4122-9.
- [28] Baskaran D, Mays JW, Bratcher MS. Noncovalent and Nonspecific Molecular Interactions of Polymers with Multiwalled Carbon Nanotubes. *Chem Mater* 2005; 17(13):3389-97.
- [29] Ajayan PM, Tour JM. Materials Science: Nanotube composites. *Nature* 2007; 447(7148):1066-8.
- [30] Bokobza L. Multiwall carbon nanotube elastomeric composites: A review. *Polymer* 2007; 48(17):4907-20.
- [31] Grady BP, Paul A, Peters JE, Ford WT. Glass Transition Behavior of Single-Walled Carbon Nanotube-Polystyrene Composites. *Macromolecules* 2009; 42(16):6152-8.
- [32] Yang Y, Xie X, Wu J, Mai Y-W. Synthesis and self-assembly of polystyrene-grafted multiwalled carbon nanotubes with a hairy-rod nanostructure. *J Polym Sci Part A: Polym Chem* 2006; 44(12):3869-81.
- [33] Nan C-W, Birringer R, Clarke DR, Gleiter H. Effective thermal conductivity of particulate composites with interfacial thermal resistance. *J Appl Phys* 1997; 81(10):6692-9.
- [34] Nan CW, Shi Z, Lin Y. A simple model for thermal conductivity of carbon nanotube-based composites. *Chem Phys Lett* 2003; 375(5-6):666-9.
- [35] Pollack GL. Kapitza Resistance. *Rev Mod Phys* 1969; 41(1):48.
- [36] Zhong H, Lukes JR. Interfacial thermal resistance between carbon nanotubes: Molecular dynamics simulations and analytical thermal modeling. *Phys Rev B* 2006; 74(12):125403.
- [37] Martelli V, Toccafondi N, Ventura G. Low-temperature thermal conductivity of Nylon-6/Cu nanoparticles. *Physica B* 2010; 405(20):4247-9.
- [38] O'Connell MJ. *Carbon Nanotubes, Properties and Applications*. Boca Raton: CRC Press; 2006: 215.
- [39] Tonpheng B, Yu J, Andersson O. Thermal Conductivity, Heat Capacity, and Cross-Linking of Polyisoprene/Single-Wall Carbon Nanotube Composites under High Pressure. *Macromolecules* 2009; 42(23):9295-301.
- [40] Peters JE, Papavassiliou DV, Grady BP. Unique Thermal Conductivity Behavior of Single-Walled Carbon Nanotube-Polystyrene Composites. *Macromolecules* 2008; 41(20):7274-7.
- [41] Grossiord N, Miltner HE, Loos J, Meuldijk J, Van Mele B, Koning CE. On the Crucial Role of Wetting in the Preparation of Conductive Polystyrene-Carbon Nanotube Composites. *Chem Mater* 2007; 19(15):3787-92.
- [42] Flory AL, Ramanathan T, Brinson LC. Physical Aging of Single Wall Carbon Nanotube Polymer Nanocomposites: Effect of Functionalization of the Nanotube on the Enthalpy Relaxation. *Macromolecules* 2010; 43(9):4247-52.

- [43] Broido DA. Length Dependence of Carbon Nanotube Thermal Conductivity and the "Problem of Long Waves". *Nano Lett* 2005; 5(7):1221-5.
- [44] Choy CL, Young K. Thermal conductivity of semicrystalline polymers -- a model. *Polymer* 1977; 18(8):769-76.
- [45] Choy CL. Thermal conductivity of polymers. *Polymer* 1977; 18(10):984-1004.
- [46] Zhou H, Zhang S, Yang M. The thermal conductivity of Nylon 6/clay nanocomposites. *J Appl Polym Sci* 2008; 108(6):3822-7.